

To which densities is spin-polarized neutron matter a weakly interacting Fermi gas?

T. Krüger,^{1,2,*} K. Hebeler,^{1,2,†} and A. Schwenk^{1,2,‡}

¹*Institut für Kernphysik, Technische Universität Darmstadt, 64289 Darmstadt, Germany*

²*ExtreMe Matter Institute EMMI, GSI Helmholtzzentrum für Schwerionenforschung GmbH, 64291 Darmstadt, Germany*

We study the properties of spin-polarized neutron matter at next-to-next-to-next-to-leading order in chiral effective field theory, including two-, three-, and four-neutron interactions. The energy of spin-polarized neutrons is remarkably close to a non-interacting system at least up to saturation density, where interaction effects provide less than 10% corrections. This shows that the physics of neutron matter is similar to a unitary gas well beyond the scattering-length regime. Implications for energy-density functionals and for a possible ferromagnetic transition in neutron stars are discussed. Our predictions can be tested with lattice QCD, and we present results for varying pion mass.

PACS numbers: 21.65.Cd, 12.39.Fe, 21.30.-x, 26.60.-c

Introduction.— Due to the large neutron-neutron scattering length, the physics of neutron matter exhibits properties similar to a unitary Fermi gas [1–3]. The energy of neutron matter is approximately 0.4 times the energy of a free Fermi gas, and neutrons form an S -wave superfluid for densities almost up to saturation density, for recent reviews see Refs. [3, 4]. These benchmark results, combined with the possibility to simulate low-density neutron matter with ultracold atoms near a Feshbach resonance [5], have led to the inclusion of ab initio results for neutron matter into modern energy-density functionals for nuclei [6, 7] and into predictions for neutron stars [8, 9]. Neutron matter is also interesting theoretically, because all many-body forces among neutrons are predicted in chiral effective field theory (EFT) to next-to-next-to-next-to-leading order (N^3 LO) [10, 11].

In this Letter, we study the properties of spin-polarized neutron matter at N^3 LO in chiral EFT [12], including consistently two- (NN), three- (3N), and four-neutron (4N) interactions. Spin-polarized neutron matter may exist in very strong magnetic fields as they occur in the interior of magnetars. For a unitary Fermi gas, the spin-polarized system is a non-interacting gas, so we ask the question to which densities spin-polarized neutrons behave like a weakly interacting Fermi gas? While the answer is simple at low densities relevant to ultracold atoms, because P -wave interactions between neutrons are weaker and many-body forces are suppressed by a power of the density, we find the surprising result (see Fig. 1 for a preview) that the energy of spin-polarized neutrons is close to a non-interacting system at least up to saturation density $n_0 = 0.16 \text{ fm}^{-3}$, which is well beyond the large S -wave scattering-length regime $n \lesssim n_0/100$. Spin-polarized neutron matter has been studied before, e.g., in Refs. [13–16], however with NN interactions only, and without a focus on the subnuclear density region and the comparison to a weakly interacting Fermi gas.

The physics of spin-polarized neutron matter is interesting, because it can provide an additional anchor point for energy-density functionals. To this end, we explore how our results compare with state-of-the-art function-

als. In addition, spin-polarized matter is ferromagnetic, so that its energy compared to the spin-symmetric system determines whether a ferromagnetic transition in neutron stars is possible [13, 14]. Finally, there are fewer non-trivial contractions for spin-polarized neutrons, so that the determination of this system is easier in lattice QCD than symmetric matter [17]. Therefore, we also study how our results depend on the pion mass and provide predictions that can be tested and refined with lattice QCD.

Computational details.— We employ the N^3 LO NN po-

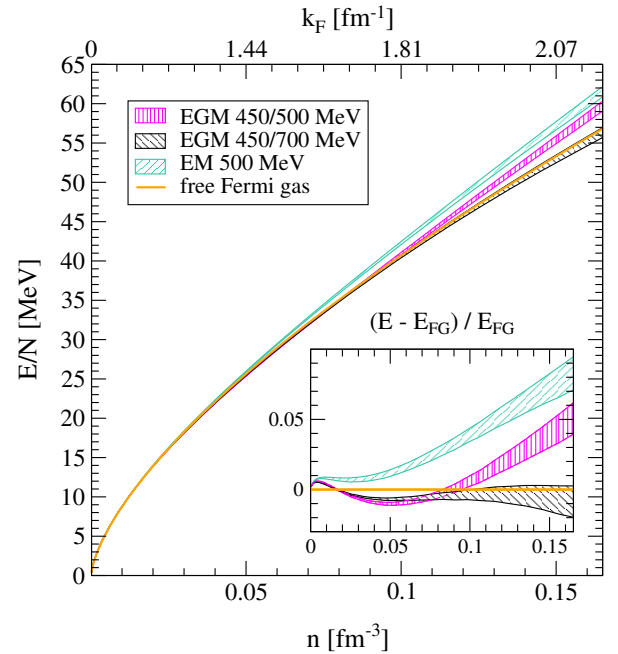


FIG. 1. (Color online) Energy per particle of spin-polarized neutron matter at N^3 LO as a function of density for the different EM/EGM NN potentials and including 3N and 4N interactions. The bands provide an estimate of the uncertainty in 3N forces and in the many-body calculation (see text). The solid (orange) line is the energy of a free Fermi gas (FG). The inset shows the relative size of the interaction contributions.

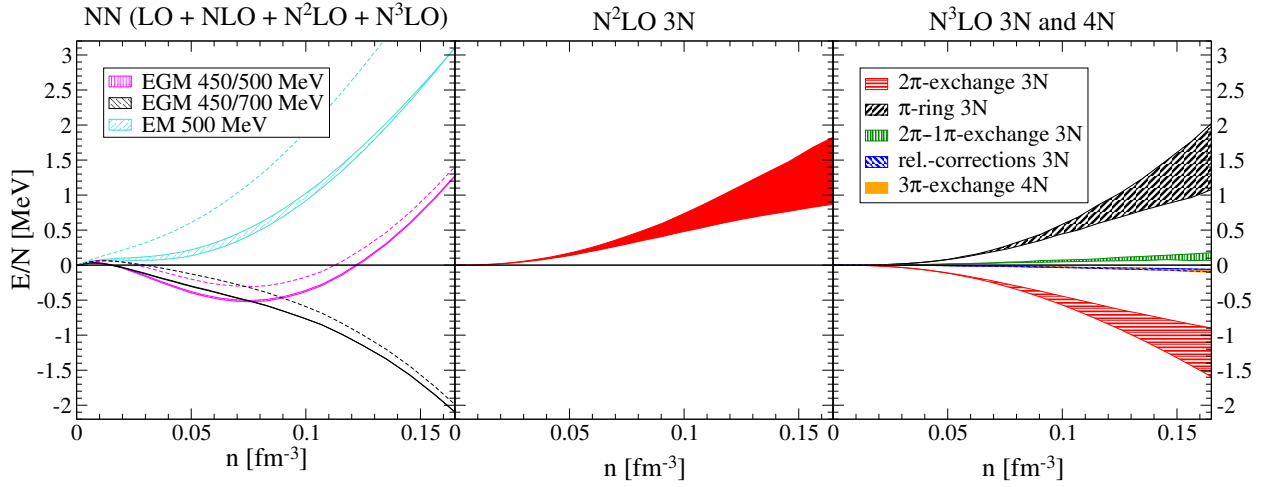


FIG. 2. (Color online) Interaction contributions at $N^3\text{LO}$ to the energy per particle of spin-polarized neutron matter as a function of density. The left panel shows the NN contributions for the three NN potentials. The width of the bands is given by the difference between second- and third-order contributions in the many-body calculation. The dashed lines are the Hartree-Fock energies. The middle panel shows the contribution from $N^2\text{LO}$ 3N forces, where the band corresponds to the range of c_i couplings used and the 3N cutoff variation $\Lambda = 2 - 2.5 \text{ fm}^{-1}$. The right panel gives the different $N^3\text{LO}$ 3N and 4N contributions, with corresponding c_i and cutoff variations. The 4N contributions overlap with the relativistic-corrections 3N energies.

tential of Entem and Machleidt (EM) with a cutoff 500 MeV [18], and the potentials developed by Epelbaum, Glöckle, and Meißner (EGM) with cutoffs $\Lambda/\tilde{\Lambda} = 450/500$ and $450/700$ MeV [19]. In this way, we explore a natural cutoff range in Weinberg’s power-counting scheme, although these potentials are not renormalizable for higher cutoffs [20]. In Refs. [11, 21], it was found that the employed potentials are perturbative in neutron matter as a result of weaker tensor forces among neutrons and restricted phase space due to Pauli blocking at finite densities. This has also been nonperturbatively verified with quantum Monte Carlo calculations using local chiral potentials [22]. Spin-polarized matter is expected to converge even faster, because S -wave interactions among polarized neutrons vanish, P -wave interactions are weaker, and Pauli blocking becomes even more effective due to the larger Fermi momentum for a given density compared to spin-symmetric matter.

We include all NN contributions up to second order in many-body perturbation theory, as well as particle-particle/hole-hole diagrams to third order (see Ref. [10]). Restricting all spins to the same spin state, the second-order contribution to the energy per particle is given by

$$\frac{E_{\text{NN}}^{(2)}}{N} = \frac{1}{4} \left[\prod_{i=1}^4 \int \frac{d\mathbf{k}_i}{(2\pi)^3} \right] \frac{|\langle 12 | V_{\text{NN}} | 34 \rangle|^2 (2\pi)^3}{\varepsilon_{\mathbf{k}_1} + \varepsilon_{\mathbf{k}_2} - \varepsilon_{\mathbf{k}_3} - \varepsilon_{\mathbf{k}_4}} n_{\mathbf{k}_1} n_{\mathbf{k}_2} \times (1 - n_{\mathbf{k}_3})(1 - n_{\mathbf{k}_4}) \delta(\mathbf{k}_1 + \mathbf{k}_2 - \mathbf{k}_3 - \mathbf{k}_4), \quad (1)$$

where $n_{\mathbf{k}}$ denotes the Fermi distribution function at zero temperature and we use the short-hand notation $i \equiv \mathbf{k}_i$ in the bra and ket states. Taking a free or a Hartree-Fock spectrum for the single-particle energies $\varepsilon_{\mathbf{k}}$ changes the

results only at the 10 keV level. This indicates that the many-body calculation is very well converged, and in the following results are given with a free spectrum. In order to simplify the numerical calculations, we average over the angles of initial and final relative momenta \mathbf{k} and \mathbf{k}' :

$$\int \frac{d\hat{\mathbf{k}} d\hat{\mathbf{k}}'}{(4\pi)^2} |\langle \mathbf{k} S = 1 M_S = 1 | V_{\text{NN}} | \mathbf{k}' S = 1 M_S = 1 \rangle|^2 = \sum_{l, l', J, \tilde{J}} 4(4\pi)^2 C_{ll'}^{J\tilde{J}} \langle k | V_{1l'lJ} | k' \rangle \langle k' | V_{1l'l\tilde{J}} | k \rangle, \quad (2)$$

where $V_{Sl'lJ}$ denote the neutron-neutron partial-wave matrix elements and $C_{ll'}^{J\tilde{J}}$ is the sum of Clebsch-Gordan coefficients $C_{l_1 m_1 l_2 m_2}^{l_3 m_3}$

$$C_{ll'}^{J\tilde{J}} = \sum_M C_{l'(M-1)11}^{JM} C_{l(M-1)11}^{JM} C_{l(M-1)11}^{\tilde{J}M} C_{l'(M-1)11}^{\tilde{J}M}. \quad (3)$$

The angular-averaging approximation has been demonstrated to be reliable for spin-symmetric matter [10] and only affects the small contributions beyond Hartree-Fock.

The energy contributions from 3N and 4N forces up to $N^3\text{LO}$ [23–27] are calculated in the Hartree-Fock approximation, following the strategy used in Refs. [11, 21]. We expect this approximation to be reliable since we found only small contributions from 3N forces at second and third order in perturbation theory in spin-symmetric neutron matter [10]. In the polarized case we expect even smaller contributions due to the enhanced Pauli blocking effects. In addition to the 3N and 4N topologies that do not contribute to the neutron-matter energy (see Ref. [10, 21]) for the spin-polarized system also

the 3N N³LO two-pion-exchange–contact topology vanishes, as a consequence of the Pauli principle excluding all leading-order NN contacts C_S and C_T . Further, the 4N N³LO diagrams V^e and V^f (according to the nomenclature in Ref. [26]) do not contribute in polarized matter. The C_S/C_T dependence of the 3N N³LO relativistic-corrections interaction is negligible and results only in energy differences at the 1 keV level at saturation density. Thus, the many-body forces essentially depend only on the low-energy couplings c_1 and c_3 , which are chosen according to Ref. [28, 29]: $c_1 = -(0.75 - 1.13) \text{ GeV}^{-1}$ and $c_3 = -(4.77 - 5.51) \text{ GeV}^{-1}$ as in Refs. [11, 21]. In order to probe the cutoff dependence of our calculation we also vary the 3N/4N cutoff $\Lambda = 2 - 2.5 \text{ fm}^{-1}$.

Results and discussion.— Our central result, Fig. 1, shows that the energy of spin-polarized neutrons is close to a non-interacting system, with interaction effects providing less than 10% corrections at n_0 (see the inset). The largest dependence of our calculations is on the NN interaction used. The EM 500 MeV potential leads to weakly repulsive interactions with $E/N \approx 61.5 \text{ MeV}$ at n_0 , compared to 55.7 MeV for a free Fermi gas. Using the EGM 450/500 and 450/700 MeV potentials results in even weaker interactions with $E/N \approx 59.5 \text{ MeV}$ and $\approx 56 \text{ MeV}$, respectively. Because n_0 for polarized matter corresponds to a high Fermi momentum of 2.1 fm^{-1} , these small differences are due to the range in NN scattering predictions at these higher momenta.

At very low densities, we can also compare our results to the dilute-gas expansion [30], where the first non-vanishing contribution is at k_F^5 from the P-wave scattering length a_P , or the P-wave scattering volume a_P^3 . We have fitted the P-wave scattering length for $k_F < 0.3 \text{ fm}^{-1}$ to our equation of state and obtain a range $a_P = 0.50 - 0.52 \text{ fm}$ depending on the NN interaction used. This is consistent with $a_P = 0.44 - 0.47 \text{ fm}$ from the different NN interactions with small corrections due to Pauli blocking that render the P-wave scattering length more repulsive in the medium.

By comparing our results with the corresponding energy range for spin-symmetric matter, $E/N \approx 14 - 21 \text{ MeV}$ at n_0 [11, 21], it is clear that a phase transition to the ferromagnetic state is not possible for $n \lesssim n_0$. Further, we expect the energy of spin-polarized neutrons at higher densities to lie above the free Fermi gas due to repulsive 3N forces (see also Fig. 2). Assuming the energy of spin-polarized neutrons remains close to a free Fermi gas also for higher densities, we can use the general equation of state constraints of Ref. [31] to provide constraints for the onset of a possible ferromagnetic phase transition. Taking the three representative equations of state [31], a phase transition to a ferromagnetic state may be possible for $n/n_0 \gtrsim 6.1, 3.4,$ and 2.3 for the soft, intermediate, and stiff equations of state, respectively. Note that if more massive neutron stars are discovered, e.g., with $2.4M_\odot$, the soft case is ruled out [31].

Figure 2 shows the individual interaction contributions. All energies are small compared to the spin-symmetric system [11, 21]. The left panel shows the NN contributions for the three N³LO potentials. The different behavior can be traced to different predictions for the scattering phase shifts. The EM 500 MeV potential gives a net repulsive contribution, with $E/N \approx 3.1 \text{ MeV}$ at n_0 (5.6% relative to E_{FG}). Up to densities $n \lesssim 0.1 \text{ fm}^{-3}$ the EGM 450/500 and 450/700 MeV potentials are in good agreement and provide only $E/N \approx -0.5 \text{ MeV}$ at $n = 0.08 \text{ fm}^{-3}$, and then start to differ. The middle panel of Fig. 2 shows the contributions from the leading N²LO 3N forces. The 3N interactions are, as in the spin-symmetric case, repulsive but with much smaller energies in the range $0.8 - 1.9 \text{ MeV}$ at n_0 . In the right panel, we show all contributions from the N³LO many-body forces. The dominant contributions are from two-pion-exchange 3N forces with energies $-(0.9 - 1.6) \text{ MeV}$ at n_0 . This is almost as large as the leading contribution of the two-pion-exchange topology, and shows that one is pushing the chiral EFT expansion to the limits. However, all these 3N contributions are still small. In addition, there are repulsive contributions from pion-ring 3N forces, which contribute $1.1 - 2.1 \text{ MeV}$ at n_0 and counteract these. Finally, there are small repulsive contributions from the two-pion–one-pion-exchange 3N topology of $0.1 - 0.2 \text{ MeV}$ at n_0 , small attractive contributions from the relativistic-corrections 3N topology, while three-pion-exchange 4N interactions contribute only -0.1 MeV at n_0 . In total, the 3N+4N contributions provide a net repulsion of $E/N = 1 - 2.2 \text{ MeV}$ at n_0 . While it is known that P-wave interactions are weak it is remarkable that even contributions from many-body forces are small.

In Fig. 3 we compare our results with predictions based on state-of-the-art energy-density functionals (for early work on polarized neutron matter with Skyrme functionals see Ref. [33]), following Ref. [32]: SIII [34], SGII [35], SkM* [36], SLy4 and SLy5 [37], SkO and SkO' [38], BSk9 [39], as well as SAMi [40] and using the Gogny D1N interaction [41]. At low densities $n \lesssim 0.01 \text{ fm}^{-3}$ all functionals agree with a free Fermi gas. However, at higher densities we find significant deviations. In best agreement with our calculations are the functionals SIII, SkO, SGII, SkM*, and SLy5, whereas the latter two reproduce the free Fermi gas and the former provide small repulsive contributions. The predictions of the functionals SLy4, SAMi, BSk9, and SkO' differ significantly from our N³LO bands. Therefore, it will be interesting to use our results as additional neutron-matter constraint for modern functionals. Note that the above discussion of a possible transition to a ferromagnetic state is different to the spin instabilities caused by the polarized system to decrease unphysically in energy, as for the SkO' case.

For comparison with lattice QCD simulations, we also vary the pion mass in NN, 3N, and 4N interactions. For this estimate we only take into account the explicit pion

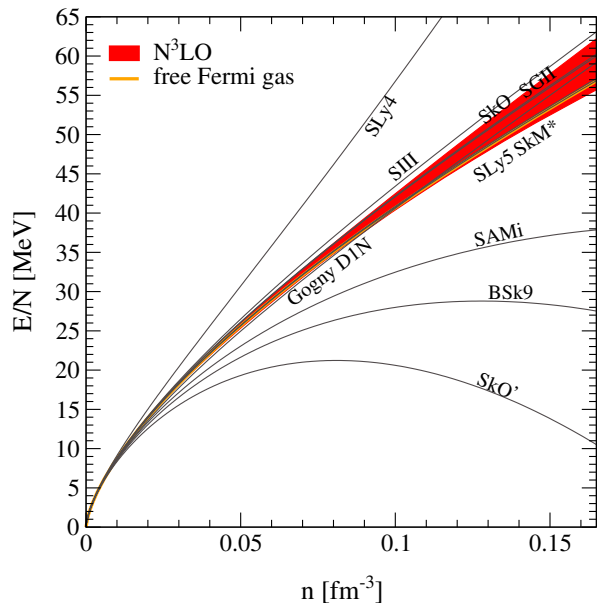


FIG. 3. (Color online) Energy per particle of spin-polarized neutron matter from Fig. 1 in comparison with different energy-density functionals (see text) following Ref. [32].

exchanges and do not vary the pion mass implicitly in the coupling constants. For spin-symmetric neutron matter, this was found to be the dominant contribution, whereas the contributions from the pion-mass dependence of the coupling constants was estimated to be smaller [42–44]. The dependence of the energy of the free Fermi gas, $E_{\text{FG}}/N = 3k_{\text{F}}^2/(10m_N)$, is a result of the change of the nucleon mass with the pion mass. This varies as [45]

$$m_N(m_\pi) = m_0 - 4c_1 m_\pi^2 - \frac{3g_A^2}{32\pi f_\pi^2} m_\pi^3 + \mathcal{O}(m_\pi^4), \quad (4)$$

where m_0 is the nucleon mass in the chiral limit and c_1 is the same low-energy coupling that enters NN and 3N forces at N²LO. We consistently also do not include the implicit pion-mass dependence of the coupling-constants in these estimates. For c_1 we use the same range above, as in the 3N forces. Using the physical values of m_N , m_π , g_A , and f_π we can extract m_0 for the employed c_1 range. This leads to the filled (orange) band in Fig. 4 at $n_0/2$ and corresponds to a range of the pion-nucleon sigma term $\sigma_{\pi N} = 34.9 - 63.9$ MeV. In Fig. 4 we show that including interactions gives a very similar m_π dependence, but away from the physical pion mass, the energy starts to deviate more from the free Fermi gas. As in spin-symmetric matter, the interaction contributions also increase the chiral condensate, as determined from the slope in m_π . We emphasize that for a precision comparison, one also needs to include the m_π dependence of the low-energy couplings in nuclear forces.

Summary and outlook.– We have presented a complete N³LO calculation of spin-polarized neutron matter,

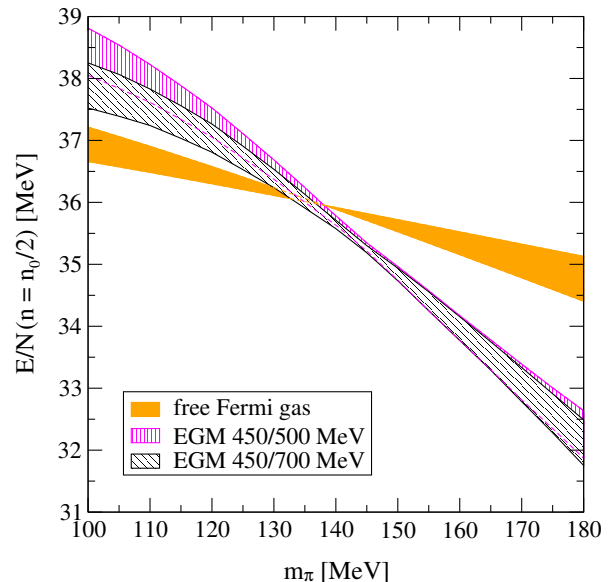


FIG. 4. (Color online) Energy per particle of spin-polarized neutron matter at a density $n = n_0/2$ as a function of the pion mass. The solid (orange) band indicates the energy of a free Fermi gas. The shaded bands correspond to the EGM NN potentials, including 3N and 4N interactions, at the same many-body calculational level as the results in Fig 1.

where the dominant uncertainty is due to the NN potential used, as well as due to the uncertainty in 3N forces. The uncertainty from the many-body calculation is very small (shown by the bands in the left panel of Fig. 2). Our results show that the energy of spin-polarized neutrons is remarkably close to a non-interacting system. This shows that the physics of neutron matter is similar to a unitary gas well beyond the scattering-length regime. Moreover, our results provide constraints for energy-density functionals of nuclei and show that a phase transition to a ferromagnetic state is not possible for $n \lesssim n_0$. Finally, our predictions can be tested and refined with lattice QCD calculations of spin-polarized neutrons in a box.

We thank W. Detmold, C. Drischler, T. Lesinski, M. Savage, and I. Tews for useful discussions. This work was supported by the DFG through Grant SFB 634, the ERC Grant No. 307986 STRONGINT, and the Helmholtz Alliance Program of the Helmholtz Association, contract HA216/EMMI “Extremes of Density and Temperature: Cosmic Matter in the Laboratory”. We thank the Institute for Nuclear Theory at the University of Washington for its hospitality and the DOE for partial support during the completion of this work.

* E-mail: thomas.krueger@physik.tu-darmstadt.de

[†] E-mail: kai.hebeler@physik.tu-darmstadt.de

[‡] E-mail: schwenk@physik.tu-darmstadt.de

- [1] J. Carlson, S.-Y. Chang, V. R. Pandharipande, and K. E. Schmidt, *Phys. Rev. Lett.* **91**, 050401 (2003).
- [2] A. Schwenk and C. J. Pethick, *Phys. Rev. Lett.* **95**, 160401 (2005).
- [3] J. Carlson, S. Gandolfi, and A. Gezerlis, *PTEP* **2012**, 01A209 (2012).
- [4] A. Gezerlis, C. J. Pethick, and A. Schwenk, arXiv:1406.6109.
- [5] I. Bloch, J. Dalibard, and W. Zwerger, *Rev. Mod. Phys.* **80**, 885 (2008).
- [6] A. Bulgac, M. M. Forbes, and P. Magierski, *Lect. Notes Phys.* **836**, 305 (2012).
- [7] S. Goriely, N. Chamel, and J. M. Pearson, *Phys. Rev. C* **88**, 061302 (2013).
- [8] K. Hebeler, J. M. Lattimer, C. J. Pethick, and A. Schwenk, *Phys. Rev. Lett.* **105**, 161102 (2010).
- [9] S. Gandolfi, J. Carlson, and S. Reddy, *Phys. Rev. C* **85**, 032801 (2012).
- [10] K. Hebeler and A. Schwenk, *Phys. Rev. C* **82**, 014314 (2010).
- [11] I. Tews, T. Krüger, K. Hebeler, and A. Schwenk, *Phys. Rev. Lett.* **110**, 032504 (2013).
- [12] E. Epelbaum, H.-W. Hammer, and U.-G. Meißner, *Rev. Mod. Phys.* **81**, 1773 (2009).
- [13] I. Vidana, A. Polls, and A. Ramos, *Phys. Rev. C* **65**, 035804 (2002).
- [14] I. Bombaci, A. Polls, A. Ramos, A. Rios, and I. Vidana, *Phys. Lett. B* **632**, 638 (2006).
- [15] F. Sammarruca and P. G. Krastev, *Phys. Rev. C* **75**, 034315 (2007).
- [16] G. H. Bordbar and M. Bigdeli, *Phys. Rev. C* **77**, 015805 (2008).
- [17] S. R. Beane, W. Detmold, K. Orginos, and M. J. Savage, *Prog. Part. Nucl. Phys.* **66**, 1 (2011).
- [18] D. R. Entem and R. Machleidt, *Phys. Rev. C* **68**, 041001(R) (2003).
- [19] E. Epelbaum, W. Glöckle, and U.-G. Meißner, *Nucl. Phys. A* **747**, 362 (2005).
- [20] A. Nogga, R. G. E. Timmermans, and U. van Kolck, *Phys. Rev. C* **72**, 054006 (2005).
- [21] T. Krüger, I. Tews, K. Hebeler, and A. Schwenk, *Phys. Rev. C* **88**, 025802 (2013).
- [22] A. Gezerlis, I. Tews, E. Epelbaum, S. Gandolfi, K. Hebeler, A. Nogga, and A. Schwenk, *Phys. Rev. Lett.* **111**, 032501 (2013).
- [23] U. van Kolck, *Phys. Rev. C* **49**, 2932 (1994).
- [24] V. Bernard, E. Epelbaum, H. Krebs, and U.-G. Meißner, *Phys. Rev. C* **77**, 064004 (2008).
- [25] V. Bernard, E. Epelbaum, H. Krebs, and U.-G. Meißner, *Phys. Rev. C* **84**, 054001 (2011).
- [26] E. Epelbaum, *Phys. Lett. B* **639**, 456 (2006).
- [27] E. Epelbaum, *Eur. Phys. J. A* **34**, 197 (2007).
- [28] M. C. M. Rentmeester, R. G. E. Timmermans, and J. J. de Swart, *Phys. Rev. C* **67**, 044001 (2003).
- [29] H. Krebs, A. Gasparyan, and E. Epelbaum, *Phys. Rev. C* **85**, 054006 (2012).
- [30] H.-W. Hammer and R. J. Furnstahl, *Nucl. Phys. A* **678**, 277 (2000).
- [31] K. Hebeler, J. M. Lattimer, C. J. Pethick, and A. Schwenk, *Astrophys. J.* **773**, 11 (2013).
- [32] M. M. Forbes, A. Gezerlis, K. Hebeler, T. Lesinski, and A. Schwenk, *Phys. Rev. C* **89**, 041301 (2014).
- [33] M. Kutschera and W. Wójcik, *Phys. Lett. B* **325**, 271 (1994).
- [34] M. Beiner, H. Flocard, N. van Giai, and P. Quentin, *Nucl. Phys. A* **238**, 29 (1975).
- [35] N. van Giai and H. Sagawa, *Phys. Lett. B* **106**, 379 (1981).
- [36] J. Bartel, P. Quentin, M. Brack, C. Guet, and H.-B. Håkansson, *Nucl. Phys. A* **386**, 79 (1982).
- [37] E. Chabanat, P. Bonche, P. Haensel, J. Meyer, and R. Schaeffer, *Nucl. Phys. A* **635**, 231 (1998); *ibid.* **643**, 441(E) (1998).
- [38] P. G. Reinhard, D. J. Dean, W. Nazarewicz, J. Dobaczewski, J. A. Maruhn, and M. R. Strayer, *Phys. Rev. C* **60**, 014316 (1999).
- [39] S. Goriely, M. Samyn, J. M. Pearson, and M. Onsi, *Nucl. Phys. A* **750**, 425 (2005).
- [40] X. Roca-Maza, G. Colò, and H. Sagawa, *Phys. Rev. C* **86**, 031306 (2012).
- [41] F. Chappert, M. Girod, and S. Hilaire, *Phys. Lett. B* **668**, 420 (2008).
- [42] N. Kaiser and W. Weise, *Phys. Lett. B* **671**, 25 (2009).
- [43] A. Lacour, J. A. Oller, and U.-G. Meißner, *J. Phys. G* **37**, 125002 (2010).
- [44] T. Krüger, I. Tews, B. Friman, K. Hebeler, and A. Schwenk, *Phys. Lett. B* **726**, 412 (2013).
- [45] J. C. Berengut, E. Epelbaum, V. V. Flambaum, C. Hanhart, U.-G. Meißner, J. Nebreda, and J. R. Peláez, *Phys. Rev. D* **87**, 085018 (2013).